DIRECT 3D NUMERICAL SIMULATION OF GRAVITATIONAL TURBULENT MIXING WITH REGARD TO MOLECULAR VISCOSITY

Stadnik A.L., Statsenko V.P., Yanilkin Yu.V.

Paper to be presented at the International Workshop on Physics of Compressible Turbulent Mixing (Cambridge, July 2004)

The paper describes computational investigation of the effect of molecular viscosity on gravitational turbulent mixing development at a plane interface of two incompressible fluids (gases) using 3D TREK code. Computation results are compared to those with no consideration of viscosity and the corresponding available data of experiments.

Turbulent mixing under Rayleigh-Taylor instability is a classic problem. There is a large amount of experimental data (see, for example, Refs.[1-2]) on TMZ growth laws for the given problem that, however, gives significantly different values of the zone growth coefficient for a section which is assumed to be self-similar ($0.04<\alpha<0.35$).

It is shown in our papers [3-5] that, similarly to the experiments, initial non-self-similar phase of turbulent mixing evolution takes place in 3D computations by TREK code without consideration of molecular viscosity. The corresponding area width depends on the difference scheme in use and the number of computational cells involved in computations and this fact points to the significant effect of scheme viscosity on the resultant solution.

Basing on the analysis of the experimental data (see Refs.[6,8]) it is shown in Ref.[7] that molecular viscosity plays a significant role in the initial turbulent mixing phase.

The present paper gives the results of 3D computations with molecular viscosity for which simulation the method of solving Navier-Stokes equations for a compressible fluid has been developed and implemented in TREK code. A series of computations with this method has been carried out using a computational grid of $N=2_{10}{}^6$ cells.

The results of computations using the techniques developed are compared to the similar ones obtained with no viscosity thus allowing us to estimate its influence both on the problem solution and the value of scheme effects.

1. Setting up computations. The problem is set similar to that of Ref.[5]: at initial time two half-spaces separated by plane $z=z_c=0$ are filled with rest ideal gases of densities $\rho_2=n\rho_1=3$ and $\rho_1=1$, Atwood number is A=0.5. Gravitational acceleration $g_z= -1\equiv -g$ is directed from a heavy substance to a light one.

The computational domain is a parallelepiped with a vertical edge of its lateral face $L_z=2$. The parallelepiped's horizontal face is a square with side $L_x=1$. The computational grid is

uniform with 100x100x200 cells in x, y, z directions, respectively. Random density perturbations are specified at the interface (in a one cell thick layer) at initial time: $\sigma\rho=\pm\rho_1\sigma$, where $\sigma=0.1$.

The initial pressure profile was specified basing on the requirement of hydrostatic equilibrium: $p(z) = p_0 - \int_{z_2}^{z} \rho(z) \cdot g \cdot dz$. Here, the upper edge coorinate is $z_2=0.875$ and the lower edge coordinate is $z_1= -1.125$; $p_0=5$. Such value of pressure p_0 is taken to meet the requirement of incompressibility for the given turbulent flow: $k=\xi L_t g << \gamma p/\rho$, where $\xi=const<<1$, $L_t<\Lambda$, L_t is the turbulent mixing zone (TMZ) width, k is turbulent energy. However, the value of p_0 is taken less than that adopted in Ref.[5] ($p_0=20$) in order to save computer time.

The equation of state of ideal gas with adiabatic constant $\gamma=1.4$ is taken. Boundary condition of "rigid wall" type with slipping was specified for all boundaries of the computational domain.

Calculations were performed with the following variations of the dynamic molecular viscosity, ν: $\nu=0$, $\nu=5\cdot10^{-3}$, $\nu=5\cdot10^{-4}$, $\nu=5\cdot10^{-5}$, $\nu=5\cdot10^{-6}$.

2. 3D computation results: integral characteristics.

Fig.1(a-d) shows the dynamics of turbulent mixing in the form of isosurfaces of volume concentrations at times t=1.2, 2.4, 4, 5 μs in computations with dynamic molecular viscosity values $\nu=0$ and $\nu=5\cdot10^{-3}$.

Fig.2 (a-d) shows raster images of volume concentrations in cross-section X=0.5 for the same computations and the same times.

One can clearly see from Figs.1, 2 the effect of molecular viscosity on mixing process, namely: the small-scale spectrum in TMZ becomes significantly weaker, as viscosity increases. In general, the flow evolution observed in computations is similar to that in previous computations with no viscosity (see Refs.[1-]5): vortexes enlarge with time and self-similar mode attainment is observed.

Self-similar mode for the given problem means, in particular, that linear time dependence of TMZ width function, $L_t(t)$ has been achieved.

$$F \equiv \frac{1}{t_0}\sqrt{\frac{L_t}{Ag}}. \qquad (1)$$

Further, time τ is measured in terms of $t_0 \equiv \sqrt{\frac{L_x}{g}}$, $(\tau \equiv t/t_0)$, and $L_t(t)$ (the width of mixing zone) is determined, as follows:

$$L_t \equiv z_2 - z_1, \qquad (2)$$

where $\beta_2(z_1)=0.02$, $\beta_2(z_2)=0.98$, β_2 is the volume fraction of the material of density ρ_2 at initial time.

Angle of inclination $dF/d\tau$ determines (see Refs.[4,5]) the adjusted value of TMZ width, $\alpha = \left(\frac{dF}{d\tau}\right)^2$ characterizing the rate of TMZ growth, in the self-similar phase

$$\alpha_a = \frac{L_t}{Agt^2} = const\,. \qquad (3)$$

Fig. 3 shows $F(\tau)$ curves obtained in computations using formula (2). One can see that within the range of rather small viscosity values, $\nu \le 5\cdot 10^{-5}$ (the corresponding Reinolds number determined similar to Ref. [7] is $\mathrm{Re}_\nu = \frac{g^2t^3}{\nu}$, $\mathrm{Re}_\nu \sim 0.5\div 4\cdot 10^6$ for t=3-6) results of computations with $\nu=5\cdot 10^{-5}$ and $\nu=5\cdot 10^{-6}$ are close to each other and to the results of computations with no viscosity considered. This means that introduction of molecular viscosity $\nu \le 5\cdot 10^{-5}$ into 3D computations gives the effect comparable to or less than the scheme viscosity. Only molecular viscosity of value $\nu > 5\cdot 10^{-5}$ exceeds the scheme viscosity in its effect on $F(\tau)$.

For $\nu \le 5\cdot 10^{-5}$, self-similar mixing stage is achieved. Fig. 3 shows similar data from Ref. [5], as well as approximation data with α_a=0.055. As it is seen, the approximation in the self-similar stage is very close both to Ref. [5] results and our results. However, there are noticeable fluctuations of all the values due to a higher compressibility during wave passage through TMZ, because our computations have been carried out with a smaller p_0 value for the sake of lower costs.

On the other hand, with a rather large viscosity value, $\nu \ge 5\cdot 10^{-4}$ (the corresponding Reinolds number is $\mathrm{Re}_\nu \sim 0.5\div 4\cdot 10^5$ for t=3-6), the results are clearly different from the previous versions of computations: the large is the viscosity value, the more durable becomes the initial (non-self-similar) phase with large angle of inclination $dF/d\tau$. Similarly to (1), determine the function of coordinate z_2 of the light fluid penetration into the heavy one:

$$F_2 \equiv \frac{1}{t_0}\sqrt{\frac{z_2 - z_c}{Ag}} \quad . \qquad (4)$$

Angle of inclination $\frac{dF_2}{d\tau}$ determines the adjusted value of coordinate z_2 of the light fluid penetration into the heavy one, $\alpha_2 = \left(\frac{dF_2}{d\tau}\right)^2$, in the self-similar phase

$$\alpha_2 = \alpha_{a2} = \frac{z_2 - z_c}{Agt^2} = const \tag{5}$$

Instant values are quite non-monotone, they fluctuate with time; as one can see in Fig.3, this should lead to even higher fluctuations of values α and α_2 obtained by differentiation.

Smooth the original quantities from formula (5) by averaging over the fixed time period ($\Delta t = 1.4$). The obtained results (Fig.4) show that if self-similar mode is achieved in computations with small viscosity values, we obtain $\alpha_{a2} \approx 0.025$; the corresponding straight line is plotted inFig.4.

Self-similar mode is not achieved in computations with large viscosity values, because large Reinolds numbers are inherent to this computation stage, which cannot be achieved with large viscosity values. This can be seen from Figs.5, 6 illustrating the dependence of the adjusted coordinate α_2 of light fluid penetration into heavy fluid on Re number.

The dependence is still irregular in 3D computations, though the figures show smoothed values. In the initial stage with small Re numbers we see wide spread of α_{a2} values, with the minimum values being correspondent to 3D computations with large viscosity values, $\nu \geq 5 \cdot 10^{-4}$ and the maximum values being correspondent to computations with small viscosity values, $\nu \leq 5 \cdot 10^{-5}$.

The experimental value of the adjusted coordinate α_b is $\alpha_b \approx 0.04$, according to the analysis made in Ref.[7]. Though this value is almost 2 times less than that adopted by the authors of Ref.[6], it is, however, noticeably larger than our results. The cause will be explained in the next section of the report.

Self-similar mode for the problem of interest is also characterized by attainment of the time-independent value of the quantity:

$$E_m(t) \equiv \frac{k_m}{L_t g}, \tag{6}$$

where $k_m(t) \equiv \max(\langle k \rangle(z,t))$ is the maximum (with respect to TMZ width) value of the averaged turbulent energy:

$$k(z) = \frac{\langle (u_j)^2 \rangle - \langle u_j \rangle^2}{2}, \tag{7}$$

averaging (denoted by <>) is performed over the entire horizontal cross-section z=const. As it is clearly seen from Fig.7, $E_m(\tau)$ in 3D computations with $\nu < 5 \cdot 10^{-4}$ reaches the approximately constant value, $E_m \approx E_{ma} \approx 0.03$ in all options of computations. In options with large viscosity values, E_m value appears to be noticeably lower because of an extremely overextended initial

period of such computations. Probably, in case of a large enough computational domain available, i.e. with a large number of computational cells, $E_m(\tau)$ would also start increasing after some long time period and achieve the value $E_m \approx E_{ma,}$ with a large enough Re number achieved. This is clearly seen from Fig.8 that shoes E_m versus Re.

Fig. 9 shows the time dependence for the maximum in TMZ ratio of squared density fluctuations:

$$R_m \equiv \frac{<\rho'^2>}{\rho^2} \quad . \tag{8}$$

As it follows from this figure, in the self-similar phase R_m value actually becomes constant (with insignificant fluctuations) and close to that obtained in Ref.[5]. The larger is the value of viscosity, the later is time, when this value appears to be achieved.

3. Studying the effect of Re number. Fig. 10 shows the adjusted coordinate α_b (of the light fluid penetrated in the heavy one) versus Re number, according to our computations. The value of α_b is determined, as described in [7], using the formula:

$$\alpha_b \equiv \frac{1}{A}\frac{\partial(z_2 - z_c)}{\partial S} \ , \tag{9}$$

where $S \equiv gt^2$.

Determine Re number following the paper [7]:

$$\mathrm{Re} = \frac{g^2 t^3}{\tilde{\nu}}, \tag{10}$$

here $\tilde{\nu}$ is a mean kinematic coefficient of molecular viscosity in TMZ. Assume further that

$$\tilde{\nu} = \nu + \nu_{cx} \, . \tag{11}$$

Here ν and ν_{cx} are kinematic coefficients of the molecular and scheme viscosity, respectively.

Take for ν_{cx} the estimate from [9] (this estimate is very approximate, it is true outside interfaces only, however, at the interfaces the computational diffusion is limited by the special method of calculating interface motions):

$$\nu_{cx} = \frac{hu}{4}, \tag{12}$$

where h is the computational cell size, u is the corresponding velocity. Since the Kolmogorov spectrum of velocity fluctuations, as it will be shown below, is established on small scales, u can be estimated basing on the relation:

$$u \le \sqrt{2E_m}\left(\frac{h}{L_t}\right)^{1/3}, \tag{13}$$

that gives an overestimated value of ν_{cx}.

The dependence of the adjusted coordinate α_b (of the light fluid penetration into the heavy one) on Re number obtained from (3.1) using smoothed values is shown in Fig.10. Apparently, the maximum value, $\alpha_b \approx 0.03 \div 0.035$ is achieved with Re number increased.

In so doing, the following two points are worth of notice.

1) According to the analysis made in [7], the maximum value, $\alpha_b \approx 0.03 \div 0.035$ obtained using the equation (9) appears to be slightly lower than $\alpha_b \approx 0.04$ from the data of experiments. However, Re numbers (obtained according to formulas (10)-(13)) for which this value of α_b is achieved (Re = Re_b~10^6) appear to be several times lower than the corresponding values from [7] resultant from processing of the data of experiments: Re_b~$5 \cdot 10^6$.

2) The maximum value, $\alpha_b \approx 0.03 \div 0.035$ obtained from (9) appears to be noticeably higher than $\alpha_{a2} \approx 0.025$ obtained in Section 4 of the report basing on the analysis of $\frac{dF_2}{d\tau}$.

Probably, one of the possible causes of the difference in Re_b number values is in the overestimated scheme viscosity.

The cause of the second and, partially, of the first circumstance (which will be discussed in more details below) is in the initial non-self-similar phase which leads to an overestimated value of α_b, when using formula (9).

Note, first of all, that α_2 values obtained in Section 2 of the report as a result of analyzing the value of $\frac{dF_2}{d\tau}$ do not depend on time shift:

$$\alpha_2 = \left(\frac{dF_2}{d\tau}\right)^2. \tag{14}$$

This fact is in favor of the given method of finding the adjusted coordinate, when self-similarity has not yet been achieved (with the self-similarity achieved, the both methods give the same value, $\alpha_b = \alpha_{a2}$).

With regard to (9) and (14), it is easy to obtain

$$K \equiv \alpha_2 / \alpha_b; \qquad K = \frac{\partial(z_2 - z_c)}{\partial S} \cdot \frac{S}{(z_2 - z_c)}. \tag{15}$$

Apparently, the value of K (and also the value of α_b) appears to be dependent on the time reference point and this is unacceptable for a quantity having physical meaning. Besides, this quantity “remembers” the initial non-self-similar section. Assume that in the initial phase

quantity $a \equiv \frac{\partial(z_2 - z_c)}{\partial S}$ has a large value and then starts descending and finally achieves its constant value, as this takes place in our computations and experiments described in [6, 8]. It is evident that in this case K≤1. Indeed, assuming, for the sake of simplicity, that a=const=a_1 at S≤S_1 and a=const=$a_2 < a_1$ at S_1≤S≤S_2, we obtain K=1 at S≤S_1 and

$$K = \frac{a_2 S}{a_2 S + (a_1 - a_2) S_1} \tag{16}$$

at S≥ S_1. This is the behavior of quantities a and K (see Fig. 11) calculated in the two versions of our computations. As one can see from formula (16), the larger is the difference between the angles of inclination $a \equiv \frac{\partial(z_2 - z_c)}{\partial S}$ in the initial and self-similar phases and the large is the relative duration of the initial phase, the lower is the value of K.

As for the two circumstances mentioned above, note first that in the self-similar phase K≈0.75 (as one can see from Fig.11) and this fact can help us to explain the quantitative difference between α_b and α_{a2} obtained in our computations for this phase. Second, this could help us to explain why the value of α_b (as well as the corresponding Re_b number) in our computations is slightly less than in the experiments; this relation follows from (16), if we assume relatively long duration of the initial phase in the experiments, as compared to our computations.

4. Velocity and density fluctuation spectra. The spectrum of velocity fluctuations has been studied basing on the data of computations according to the formula:

$$\begin{aligned} &E_{iil}^{(n)}(x,y) = \langle u_i^2 \rangle_{|_{l,x,y,z}} - \langle u_i \rangle^2_{|_{l,x,y,z}} \qquad ; \qquad n = 1,2....N_z \\ &E_{iil}(z) = E_{iil}^{(n)} = \langle E_{iil}^{(n)}(x,y) \rangle \qquad ; l = rh, \qquad r = 2,3....N_x . \end{aligned} \tag{17}$$

Here, averaging $\langle\rangle_{|_{l,x,y}}$ is performed over the n-th layer (in z) in the square with side l (l=rh, h is the computational cell size), which central point has coordinates x, y, and then it is followed by averaging ($\langle\rangle$) over all possible values x, y of squares with the same l value over the entire n-th layer. Formula (17) contains no summation over **i** .

Further,

$$E_l = \sum_{i=1}^{i=3} E_{iil} \tag{18}$$

Computations results at time τ=4 are shown in Fig.12: here, computations with $\nu = 5 \cdot 10^{-6}$ are on the left side and computations with ν=0 are on the right side. Kolmogorov spectrum is also given for comparison

$$\lg E_l = -2/3 \lg K + \text{const}, \tag{19}$$

where K=2π/l. Let us recall that the spectral density of fluctuations is $\tilde{E}_K \sim E_l / K \sim K^{-5/3}$.

Fig.12 shows the adjusted coordinate value:

$$\zeta \equiv \frac{z - z_c}{L_t}, \tag{20}$$

negative values of this quantity correspond to the TMZ edge adjusting the light substance.

The total energy spectrum E_l on small scales (large K values) approaches to the 3D Kolmogorov spectrum, significant closeness is observed near the heavy substance (positive values of ζ). With large K values, some isotropization is observed: E_{iil} components become closer to each other, though insignificantly. As one can see, the density spectrum on small scales approaches to Kolmogorov spectrum, it appears to be more close to Kolmogorov spectrum near the heavy substance ($\zeta = 0.3 \div 0.5$). The spectra are qualitatively similar to each other in the both versions of computation. Inside TMZ they are also quantitatively similar, while on TMZ edges a significant quantitative difference is observed: in computation with viscosity fluctuations are smaller, as it could be expected.

A similar quantity is calculated for squared fluctuations of density:

$$\begin{aligned} &\rho_l^n(x,y) = \langle \rho^2 \rangle_{|_{l,x,y,z}} - \langle \rho \rangle^2_{|_{l,x,y,z}} \qquad ; \qquad n = 1,2....N_z \\ &\rho_l(z) \equiv \langle \rho_l^n(x,y) \rangle \qquad ; l = rh, \quad r = 2,3....N_x; \end{aligned} \tag{21}$$

it is shown in Fig.13 at time τ=4: here computations with $\nu = 5 \cdot 10^{-6}$ are on the left side and computations with ν=0 are on the right side.

As one can see, the density spectrum on small scales approaches to Kolmogorov spectrum, it appears to be more close to Kolmogorov spectrum near the heavy substance ($\zeta = 0.3 \div 0.5$). In the both versions of computations the spectra are qualitatively similar. Inside TMZ they are also quantitatively close to each other, while on TMZ edges there is a significant quantitative difference: in computation with viscosity fluctuations are smaller, as one could expect.

Conclusions. The direct 3D numerical simulation of gravitational turbulent mixing with consideration of molecular viscosity we have carried out shows the following:

- with a small enough viscosity value the results of computation are close to those without viscosity. This means the value of viscosity in such case is comparable to the scheme viscosity value. The self-similar phase of mixing has been achieved. A constant value of the adjusted coordinate of the light fluid penetration into the heavy one corresponds to this self-similar phase it characterizes the TMZ growth velocity. The maximum, in TMZ,

value of the adjusted turbulent energy, E_m and the maximum value of squared density fluctuations also remain constant in this mode;

- the curve has been constructed for the adjusted coordinate α_b of the light fluid penetration into the heavy fluid versus Re number determined by the summarized molecular and scheme viscosities. The curve is qualitatively similar to that from Ref.[7] obtained basing on the analysis of the experimental data presented in Refs.[6,8] and using Re_v : α_b value decreases, as Re increases, and reaches the maximum self-similar value;
- the definition we have adopted for the adjusted coordinate α_2 (which is more correct, on our opinion) leads to significantly lower values in the self-similar phase, as compared to the values of similar quantity α_b defined in Ref.[7]. The paper attributes this difference to availability of an initial non-self-similar section;
- the value of α_b in self-similar phase in our computations is slightly lower than in the experiments [6,8]. The corresponding Re_b number of the self-similar phase achieved is also smaller than that in Ref.[7] obtained basing on the analysis of the experimental data. The difference is attributed to a relatively long duration of the initial non-self-similar section in the data of experiments [6,8].
- with large enough molecular viscosity coefficients used in computations duration of the initial non-self-similar section increases, however, Re number which can be achieved decreases.
- Similar to computations without viscosity, the spectrum of velocity fluctuations on small scales is close to Kolmogorov's spectrum inside TMZ, however, anisotropy of diagonal components of Reinolds tensor remains significant. The spectrum of density fluctuations inside TMZ is also close to Kolmogorov's spectrum on small scales.

To conclude, it should be noted that the adjusted results have been obtained using rather coarse grids (from viewpoint of turbulent mixing simulation), so the results are considered preliminary. It is necessary to carry out a similar investigation, however, with significantly more fine grids that would allow finding more valid answers to the issues of interest.

References

1. Youngs // D.L., Phys. Fluids,1991, A3, 1312.
2. Youngs D.L., Numerical simulation of mixing by Rayleigh-Taylor and Richtmyer-Meshkov instabilites // Laser and Particle Beams. 1994. Vol. 12, No. 4. pp. 725-750.

3. Zhmailo V.A., Stadnik A.L., Statsenko V.P., Yanilkin Yu.V. Direct numerical simulation of gravitational turbulent mixing. // Physics of Compressible Turbulent Mixing, Stony Brook, 1995.
4. Zhmailo V.A., Stadnik A.L., Statsenko V.P., Yanilkin Yu.V., Sin'kova O.G. 3D Numerical Simulation of Gravitational Turbulent Mixing //Presentation at the 6th International Workshop "Physics of Compressible Turbulent Mixing". 1997. Marseilles.
5. Yanilkin Yu.V., Statsenko V.P., Rebrov S.V., Sin'kova O.G., Stadnik A.L. Study of gravitational turbulent mixing at large density differences using direct 3D numerical simulation // Presentation at the 8th International Workshop on Physics of Compressible Turbulent Mixing. 8th IWPCTM, Pasadena, USA, 2001.
6. Kucherenko Yu.A., Shestachenko O.E., Piskunov Yu.A., Sviridov E.V., Medvedev V.M., Baishev A.I. Experimental Investigation of the Self-Similar Mode of Mixing Different-Density Gases in Earth's Gravitational Field. // Presentation at the 6th Zababakhin's Scientific Talks. 24-28 September 2001. Snezhinsk. Russia.
7. Aisimov V.I., Kozlovskikh A.S., Baban' S.A. Studying the Results of Experiments on Turbulent Mixing with Moderate Reinolds Numbers in Earth's Gravitational Field.// Presentation at Zababakhin's Scientific Talks. 2003. Snezhinsk. Russia.
8. Kucherenko Yu.A., Shestachenko O.E., et al. Experimental Investigation of the Evolution of Gravitational Gas Mixing Using a Multiple-Purpose Shock Tube// Presentation at the 6th Zababakhin's Scientific Talks. 24-28 September 2001.Snezhinsk. Russia
9. Stadnik A.L., Shanin A.A., Yanilkin Yu.V. Eulerian Code TREK for 3D Gas Dynamic Multi-Material Flow Computations // VANT. Ser.: Math.Model.Phys. Process. 1994. Iss.4.

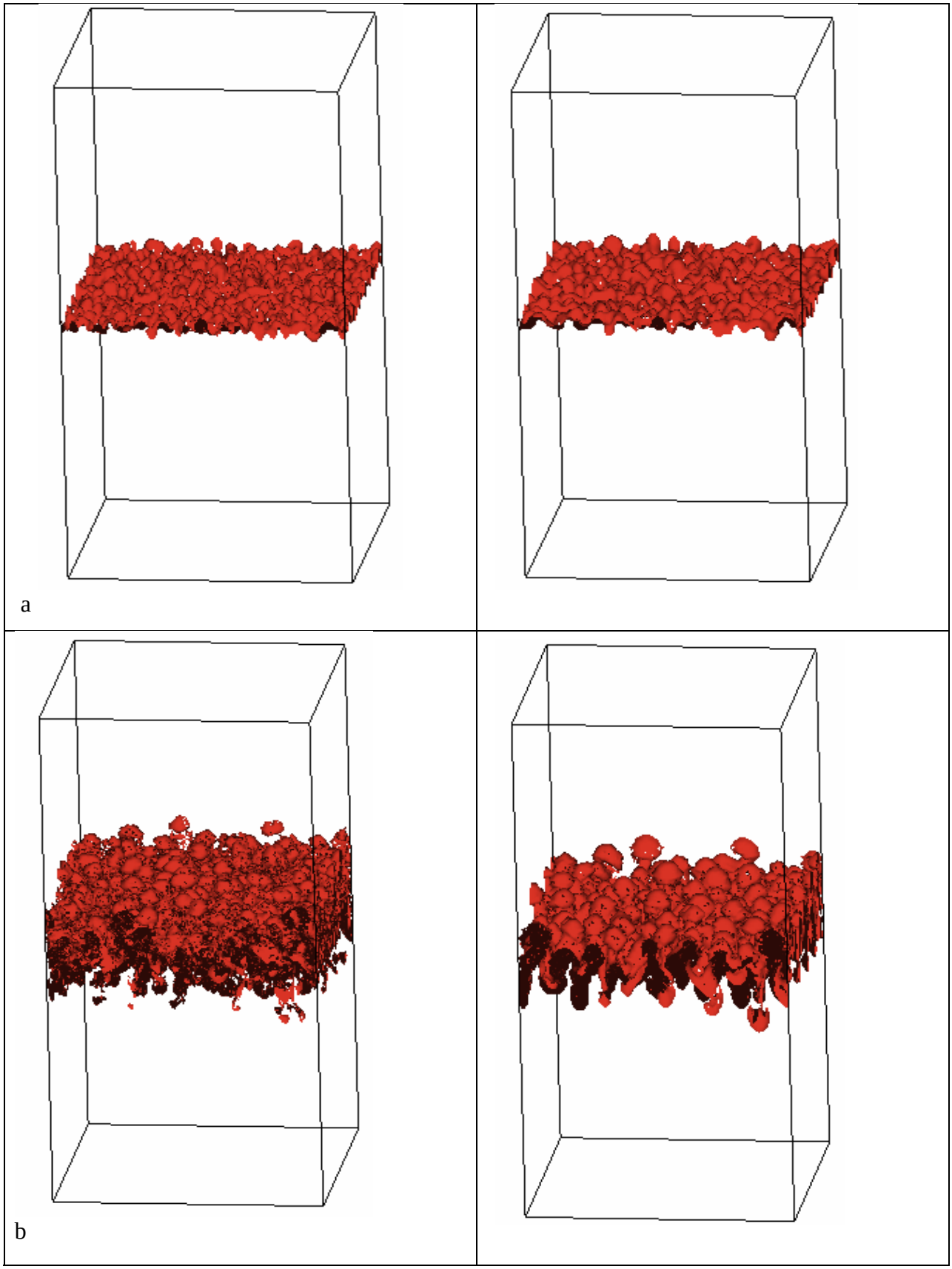
a
b
ν=0
ν=5·10⁻³

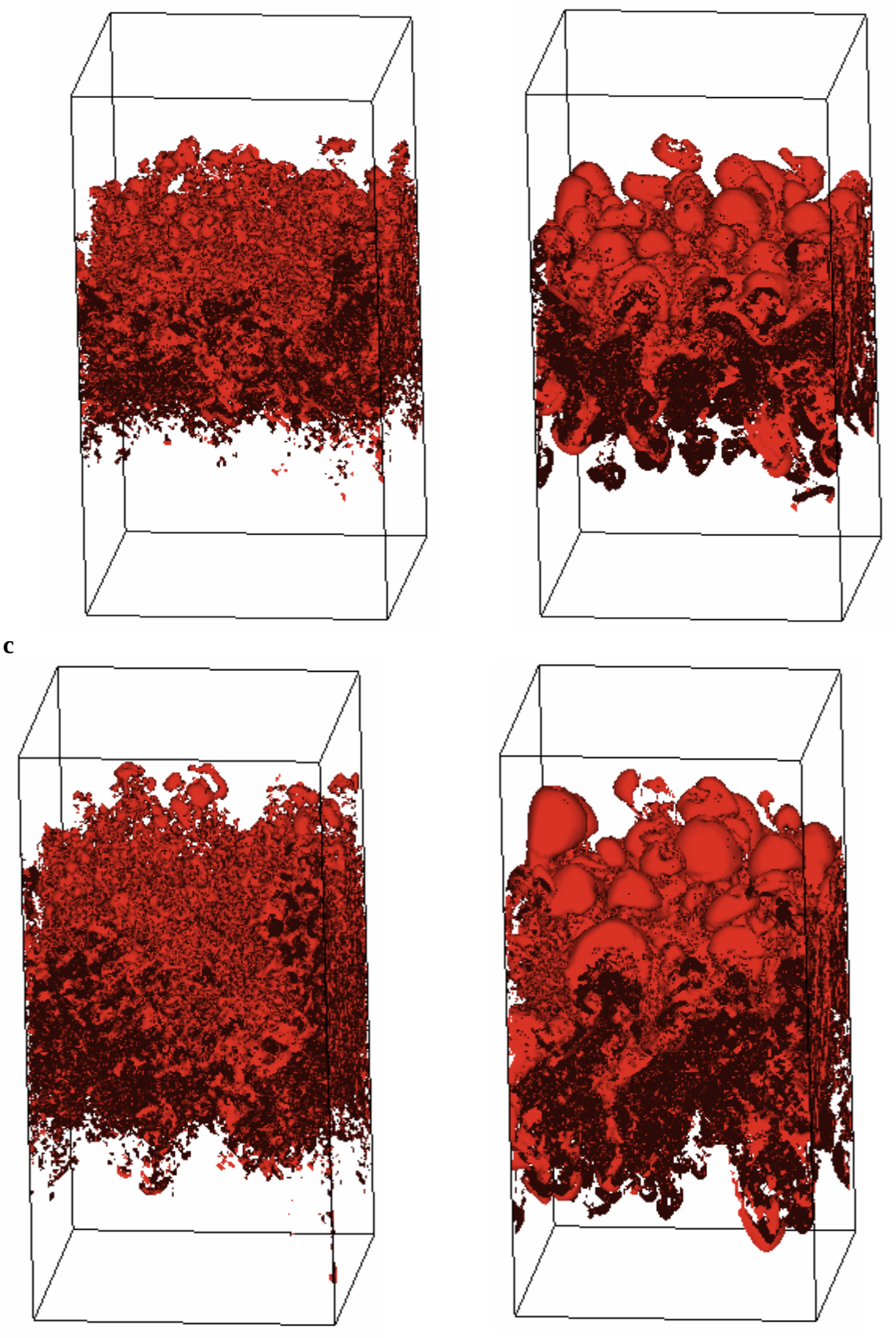

Fig. 1. Isosurfaces of volume concentrations at times t= 1.2, 2.4, 4,5 μs in computations with ν=0 and $\nu = 5 \cdot 10^{-3}$.

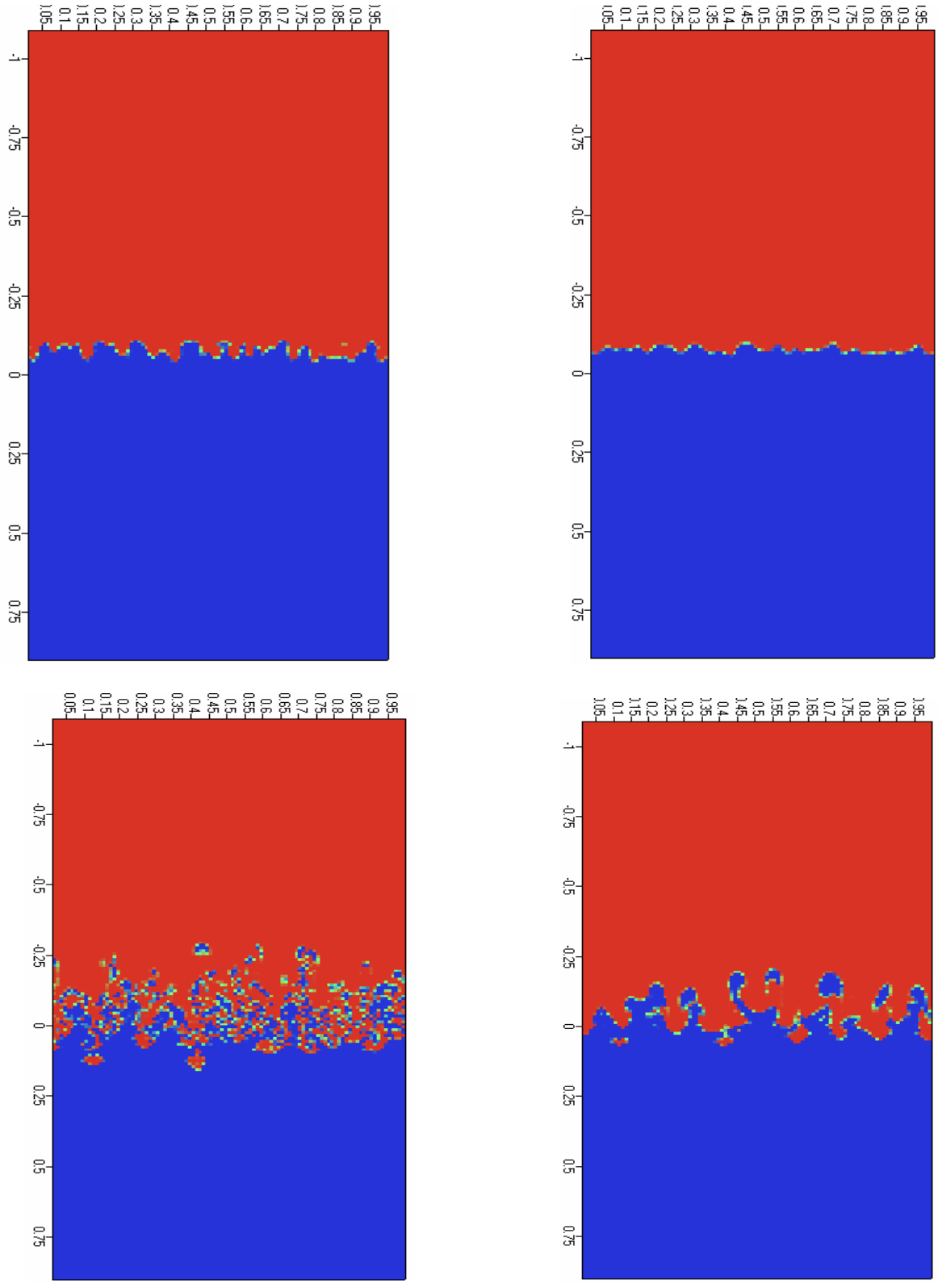

$\nu=0$ $\nu=5\cdot10^{-3}$

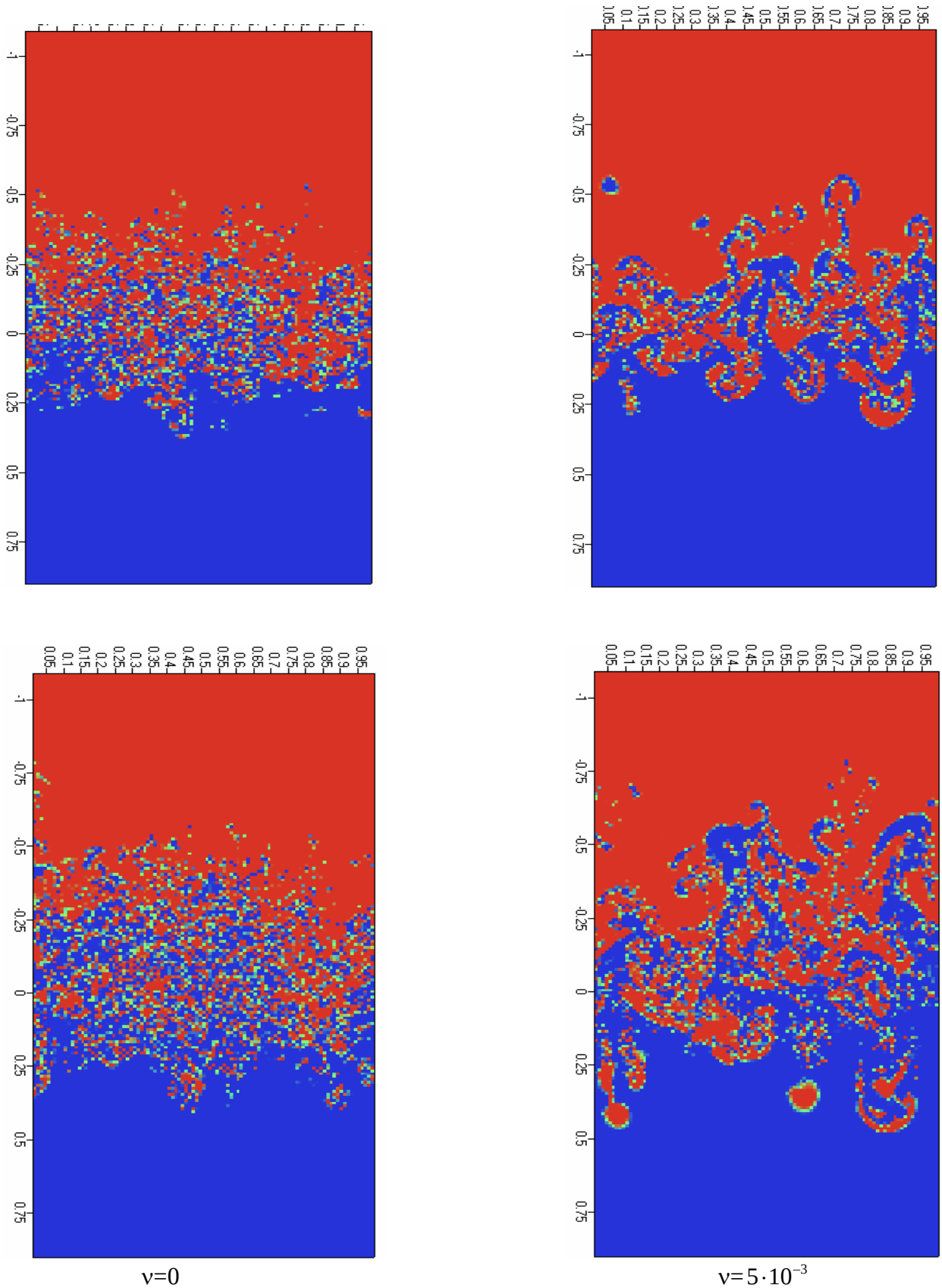

$\nu=0$ $\nu=5\cdot10^{-3}$

Fig. 2. Raster images of volume concentrations at times t= 1.2, 2.4, 4,5 μs in computations with $\nu=0$ and $\nu=5\cdot10^{-3}$.

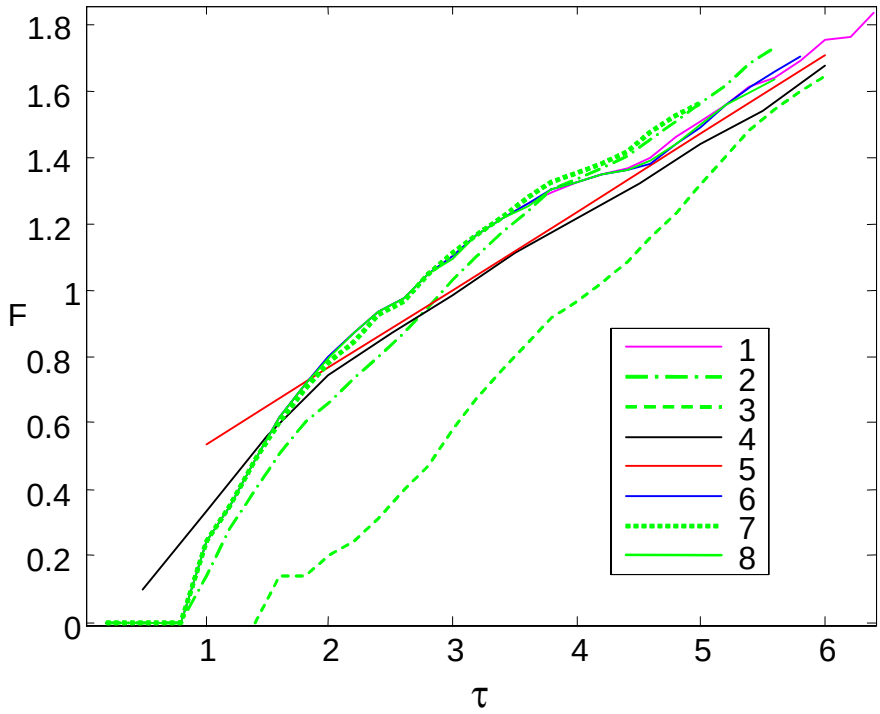

Fig. 3. The time dependence of TMZ width function in 3D computations: 1,8 – ν=0, 2 – $\nu=5\cdot10^{-4}$, 3 – $\nu=5\cdot10^{-3}$, 4 – computation [5] with ν=0 using fine grid,
6 - $\nu=5\cdot10^{-6}$, 7 - $\nu=5\cdot10^{-5}$, 5 – approximation with α_a =0.055.

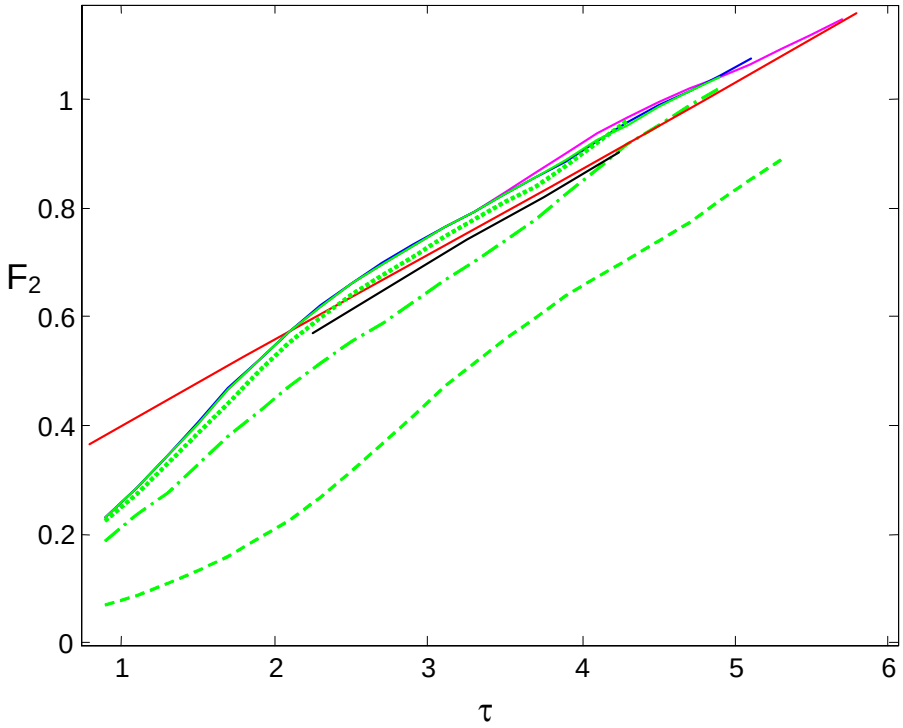

Fig.4. The smoothed dependence of the function of coordinate z_2 on time: 5 – approximation with α_a =0.025, the rest notations are the same as in Fig.3.

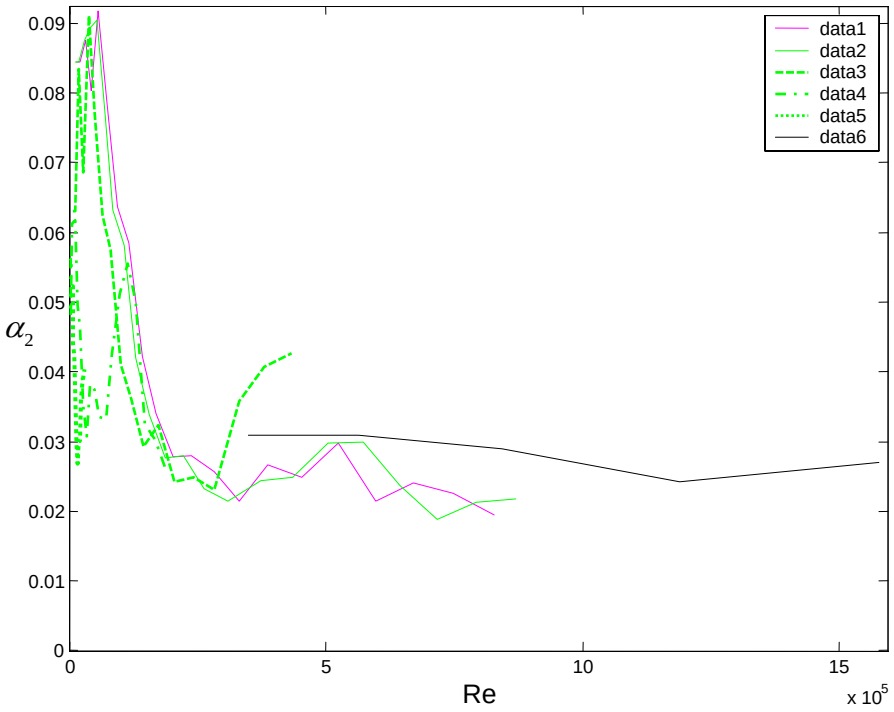

Fig.5. The smoothed dependence of the adjusted coordinate α_2 on Re number: 1 – ν=0, 2 - ν=5e-6, 3 - ν=5e-5, 4 - ν=5e-4, 5 - ν=5e-3, 6 – ν=0 (fine grid)

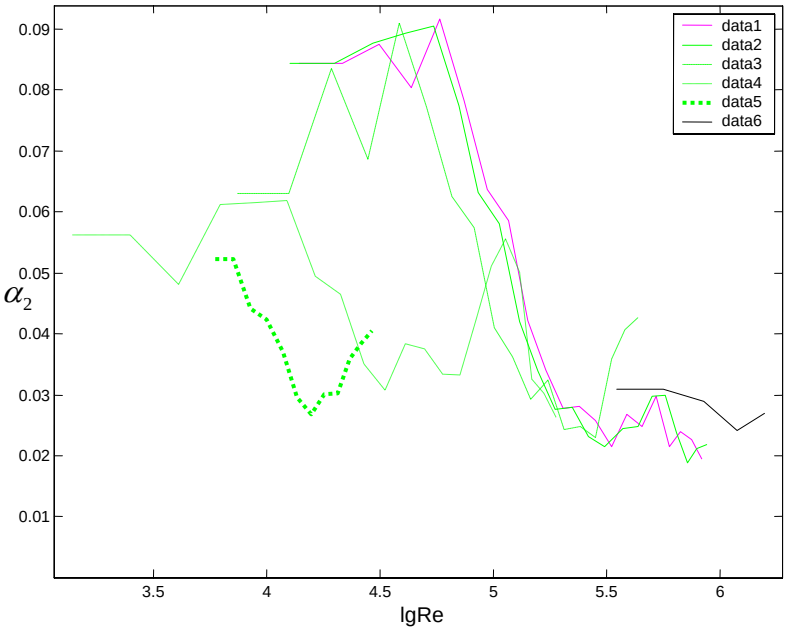

Fig.6. The smoothed dependence of the adjusted coordinate α_2 on lgRe:1 – ν=0, 2 - ν=5e-6, 3 - ν=5e-5, 4 - ν=5e-4, 5 - ν=5e-3, 6 – ν=0 (fine grid)

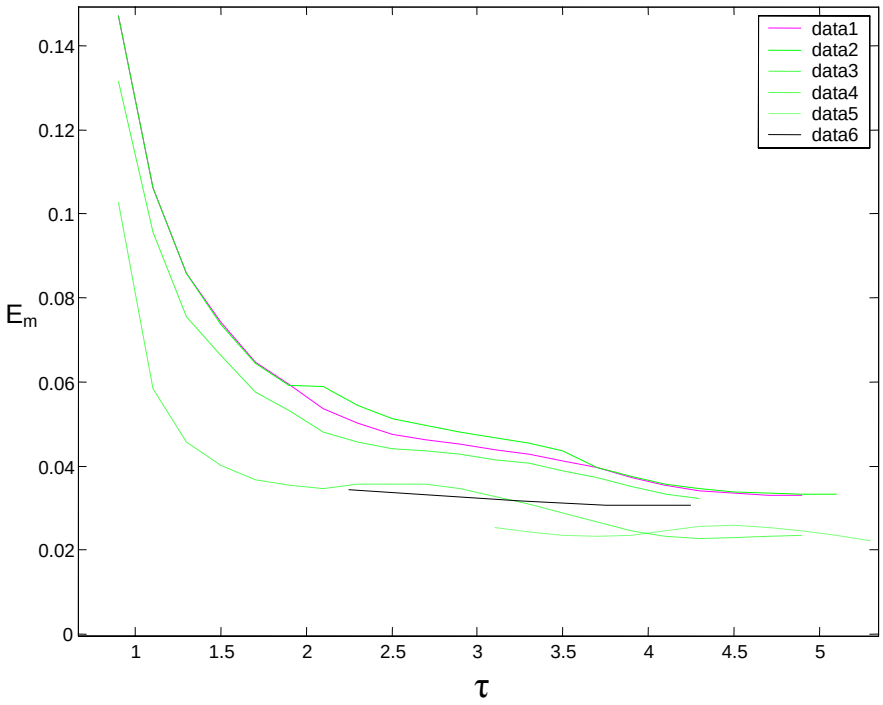

Fig.7. The maximum adjusted turbulent energy in TMZ versus time: 1 – ν=0, 2 - ν=5e-6, 3 - ν=5e-5, 4 - ν=5e-4, 5 - ν=5e-3, 6 – ν=0 (fine grid)

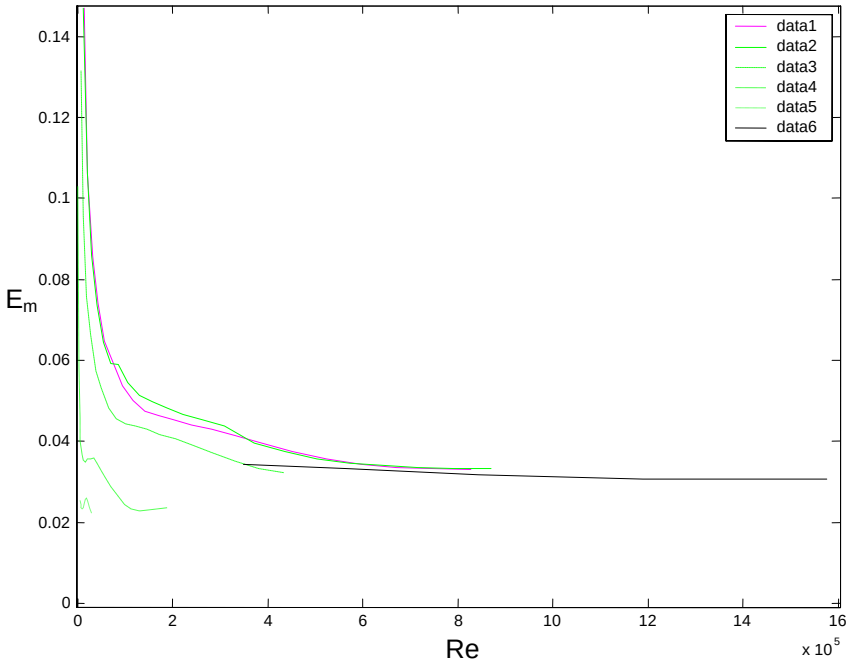

Fig.8. The maximum adjusted turbulent energy in TMZ versus Re number: 1 – ν=0, 2 - ν=5e-6, 3 - ν=5e-5, 4 - ν=5e-4, 5 - ν=5e-3, 6 – ν=0 (fine grid)

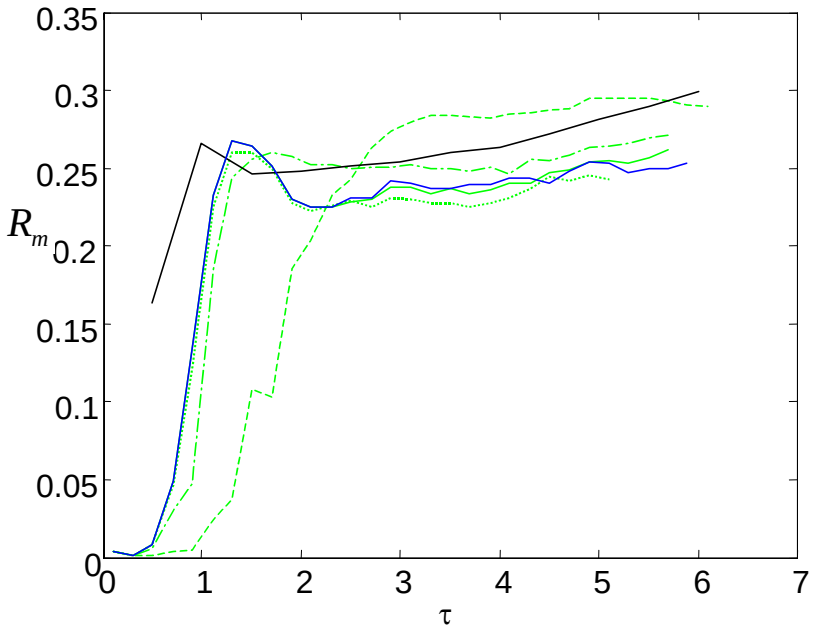

Fig.9. The time dependence for the maximum in TMZ ratio of squared density fluctuations, R_m (notations are the same as in Fig.3).

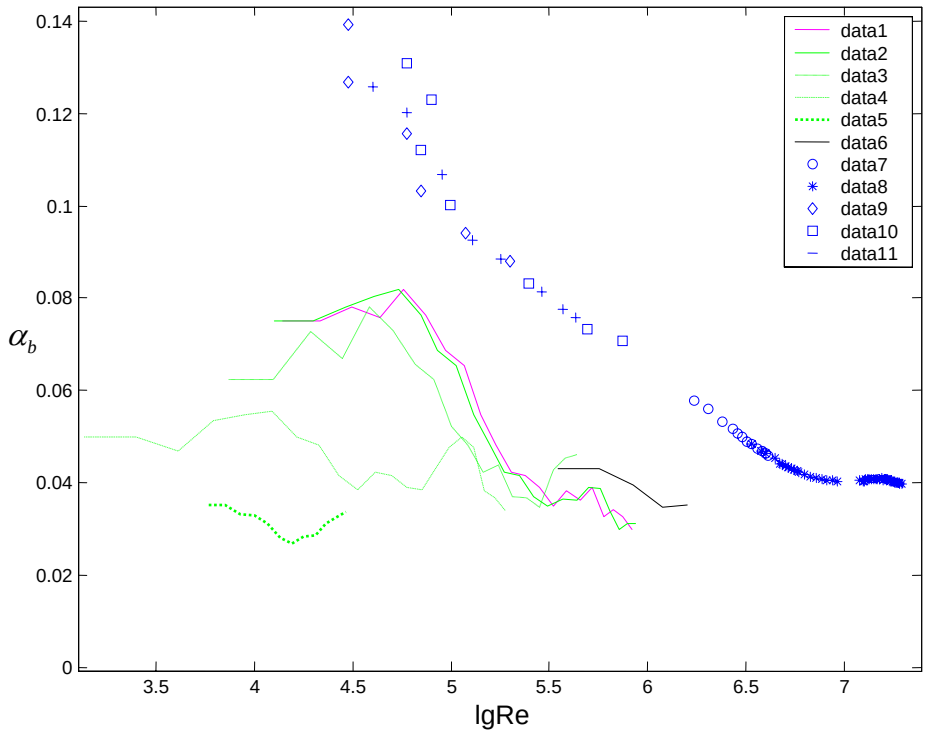

Fig.10. The smoothed value of the adjusted coordinate α_b of the light fluid penetration into the heavy fluid versus Re number.
1 – ν=0, 2 - ν=5e-6, 3 - ν=5e-5, 4 - ν=5e-4, 5 - ν=5e-3; 6 – ν=0 (fine grid);
Experiments: 7 – He-Ar [8], 8 – Ar-Kr [8], 9 – He-SF_6 [6], 10 – Ar -SF_6 [6], 11 – Ar-Kr [6].

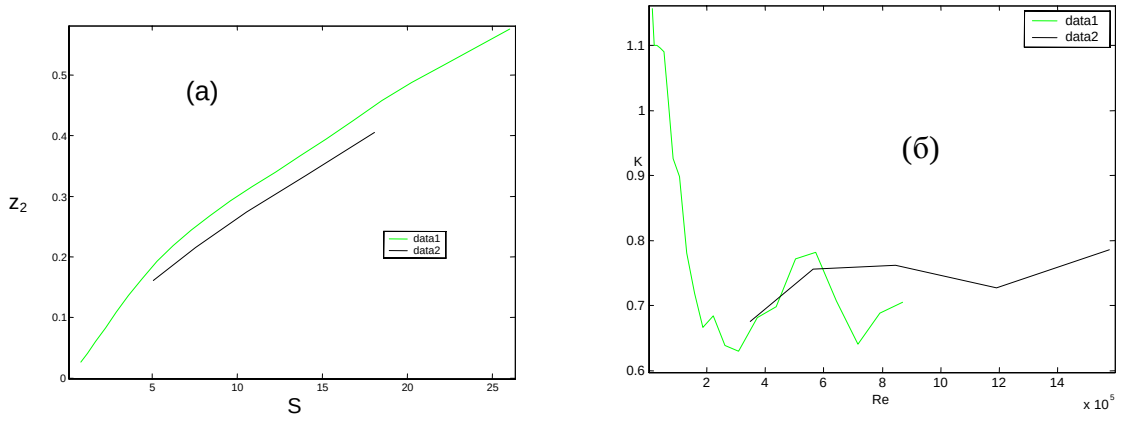

Fig.11. a) Coordinate z_2 of the light fluid penetration into the heavy fluid versus displacement S. b) The ratio of the adjusted coordinates, K, versus Re number. 1- ν=5e-6; 2 –fine grid, ν=0.

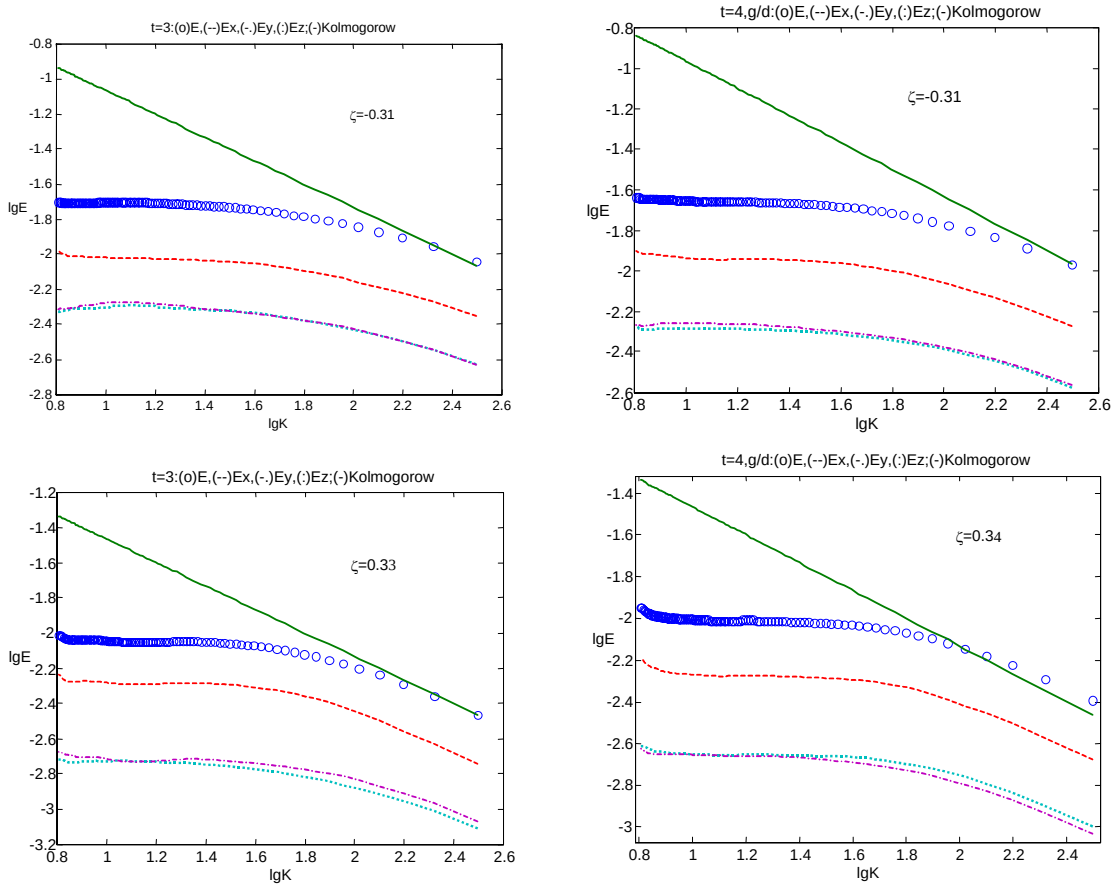

Fig.12. Thevelocity fluctuation spectrum, τ=4: on the left – computations with $\nu=5\cdot10^{-6}$, on the right – computations with ν=0: 1 – El, 4 - Exxl, 5 - Eyyl, 3 - Ezzl ; 2 –Kolmogorov spectrum.

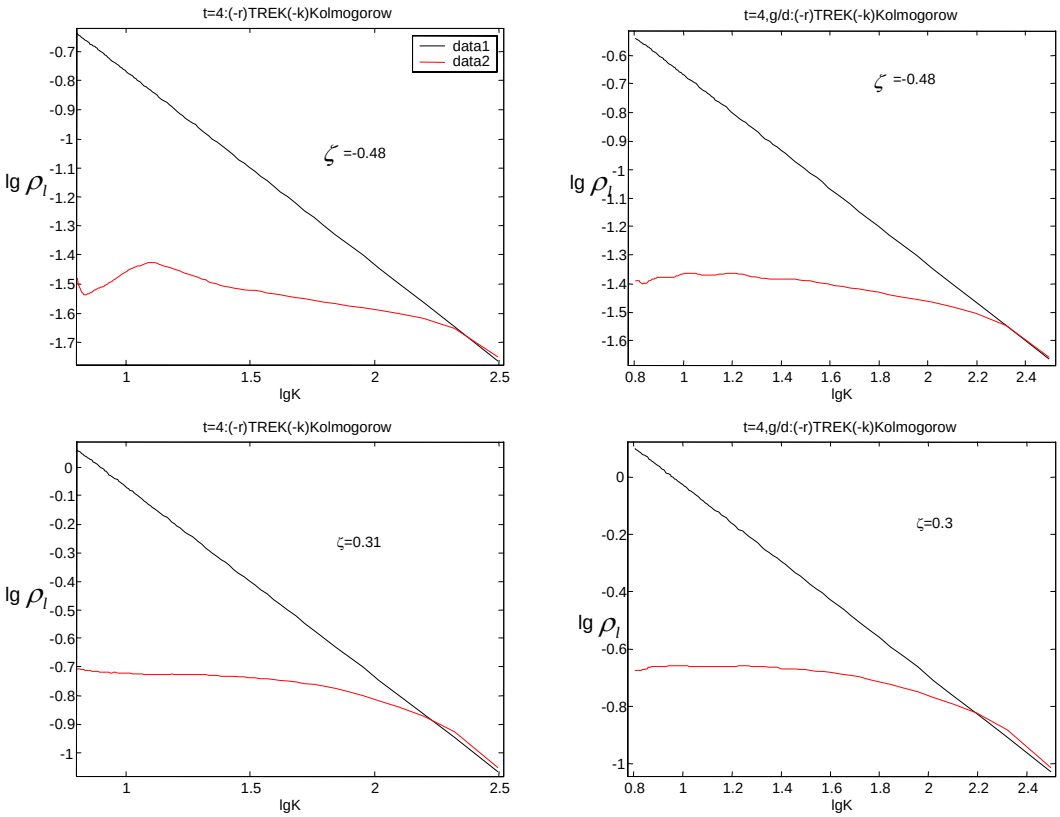

Fig.13. The density fluctuation spectrum, τ=4, computations with $\nu = 5 \cdot 10^{-6}$ (on the left) and ν=0 (on the right): 1 Kolmogorov spectrum; 2 – numerical simulation.